Biomedicine & Pharmacotherapy 158 (2023) 114175

Contents lists available at ScienceDirect

Biomedicine & Pharmacotherapy

journal homepage: www.elsevier.com/locate/biopha

Rutin ameliorates gout via reducing XOD activity, inhibiting ROS production and NLRP3 inflammasome activation in quail

Hao Wu [a,1], Yu Wang [a,1], Jingjian Huang [a], Yaolei Li [a], Zhijian Lin [a,b], Bing Zhang [a,b,*]

[a] Department of Clinical Chinese Pharmacy, School of Chinese Materia Medica, Beijing University of Chinese Medicine, Beijing, PR China
[b] Center for Pharmacovigilance and Rational Use of Chinese Medicine, Beijing University of Chinese Medicine, Beijing, PR China

ARTICLE INFO

Keywords:
Gout
Rutin
XOD
Uric Acid
ROS
NLRP3 inflammasome

ABSTRACT

Gout is a metabolic disease affected by monosodium urate (MSU) deposition, which is directly related to hyperuricemia. Recent reports on the prevalence and incidence of gout have been widely circulated worldwide. Currently, the anti-gout drugs in clinical practice are mainly small-molecule synthetic drugs, and the effectiveness and safety are limited. Reducing uric acid and inhibiting inflammation are the focused areas of drug research and development on gout. Rutin, a natural flavonoid, has been reported to alleviate inflammation in various diseases. However, whether rutin exerts protective effects on gout remains to be elucidated. This study used quails without urate oxidase as experimental animals to induce endogenous gout models through a high purine diet. We confirmed that quail in the model group developed gout symptoms at 30 days of the experiment. And the targets of uric acid metabolism, oxidative stress level, and NLRP3 inflammasome were dysregulated in quails. Rutin treatment improves gout and reduces inflammatory expression in quail. We further confirmed that rutin treatment reduced XOD activity and uric acid levels in quail. And rutin inhibited ROS production, restored oxidative stress balance, inhibited NLRP3 inflammasome activation, and exerted anti-inflammatory effects. We extracted and identified the fibroblast-like synoviocytes (FLS) for the first time. The results showed that rutin could reduce ROS production and NLRP3 inflammasome activation of FLS after uric acid stimulation. In conclusion, our findings underscore that rutin may be a gout protective agent by reducing XOD activity, inhibiting ROS production and NLRP3 inflammasome activation. Meanwhile, this study also provides an available animal model for the research drugs of gout.

1. Introduction

Gout is a metabolic disease in which the metabolism of purines is impaired, and uric acid in the blood is continuously elevated, resulting in the deposition of crystallized urate precipitates in tissues or organs, causing tissue damage. The clinical manifestations are repeated joint inflammation and dysfunction, uric acid nephropathy, and so on [1–3]. Recent reports on the prevalence and incidence of gout have been widely circulated worldwide, bringing a substantial economic burden to society [4–6].

Gout is a progressive metabolic disease closely related to hyperuricemia and urate deposition. Its disease process includes the hyperuricemia stage, urate deposition stage, and acute inflammation stage [7,8]. In 2019, the American College of Rheumatology Academic Annual Meeting 2020 Draft Gout Clinical Practice Guidelines (Draft) broke through the previous understanding that acute inflammation in gout could not be treated with urate-lowering therapy. And it pointed out that gouty arthritis should be treated with urate-lowering intervention and anti-inflammatory treatment [9]. However, most anti-gout drugs currently used in clinical practice are chemical drugs with clear targets, aiming to reduce blood uric acid and anti-inflammatory and analgesia. Although they have significant therapeutic effects, they lack the overall intervention of lowering uric acid and anti-inflammatory and have different safety risks, which makes it challenging to meet the clinical treatment needs of gout [10]. Therefore, according to the characteristics of the disease, the overall intervention of gout and safe drug development will be an essential direction for the prevention and treatment of gout in the future. In a recent study, we found that the function and

* Correspondence to: Department of Clinical Chinese Pharmacy, School of Chinese Materia Medica, Beijing University of Chinese Medicine, South Yang-Guang Road, Fang-shan District, Beijing 102488, PR China.
E-mail address: zhangb@bucm.edu.cn (B. Zhang).
[1] These authors have equally contributed to this work

https://doi.org/10.1016/j.biopha.2022.114175
Received 25 October 2022; Received in revised form 21 December 2022; Accepted 28 December 2022
Available online 30 December 2022

application value of glycans and glycosylation has gradually emerged in inflammation, especially in gout. Most glycoproteins are potential drug targets and biomarkers for disease diagnosis. Therefore, an in-depth study of the glycophorin structure of glycoprotein will eventually improve the sensitivity and specificity of a glycoprotein for the clinical detection of gout, which also provides a reference for further gout studies [11].

Rutin is a natural flavonoid compound. Studies have shown that rutin has various pharmacological activities, including myocardial protection [12–16], anti-inflammatory [17–19], antioxidant [20–24], anti-apoptosis [25–27], and other effects [28–32]. Recent studies have shown that rutin can inhibit the activity of xanthine oxidase (XOD) in vitro, the key enzyme responsible for uric acid production in the target group of uric acid metabolism [33]. Hyperuricemia is the biochemical basis of gout, and the target group of uric acid metabolism regulates its pathological process. Recent studies have found that when the XOD inhibitor is given, a significant decrease in serum interleukin-1β (IL-1β) level was observed in patients with hyperuricemia. Uric acid is the end product of purine metabolism, and the physiological concentration of uric acid is an essential antioxidant in the body, which can reduce oxidative damage caused by ROS [34,35]. Uric acid with higher than physiological concentration is mainly deposited in the form of crystals in the body tissues or organs, which can induce mitochondrial damage, promote the expression and release of ROS, activate the nucleotide-binding oligomerization domain-like receptor protein 3 (NLRP3) inflammasome, resulting in tissue and organ damage [36].

The precise pathological mechanism of gout mainly involves the release of IL-1β mediated by the NLRP3 inflammasome. As a urate-lowering and anti-inflammatory agent, the role of rutin in gout is an intriguing research topic. The uric acid metabolism of quail is similar to that of humans, and neither of them has urate oxidase in vivo, which cannot convert uric acid to allantoin. Therefore, the quail model can be used to simulate the corresponding process of the human body. The previous study of our research group showed that quail is the dominant animal model in modeling gout disease and evaluating drug efficacy [37–42]. Therefore, this study clarified the therapeutic effect of rutin on gout and investigated its mechanism. Rutin may play a role in the treatment of gout by inhibiting the activity of XOD and reducing the level of uric acid in the body, thereby improving the level of oxidative stress in the body, inhibiting the activation of ROS and NLRP3 inflammasome, reducing inflammation in the body. At the same time, fibroblast-like synoviocytes (FLS) were extracted and identified in quail for the first time. Using FLS as a vehicle for in vitro studies further confirmed our conclusions. Our findings suggest that rutin may be a promising drug for gout treatment.

2. Materials and methods

2.1. Antibodies and reagents

Rutin was purchased from Yuanye (Shanghai, China). Antibodies to NLRP3 (27458–1-AP) and GAPDH were purchased from Proteintech (Rosemont, IL, USA). Antibody to vimentin was purchased from Bioss (Beijing, China). Yeast powder (LP0021B) was purchased from Oxoid (Basingstoke, United Kingdom). D (-)-Fructose (18G3056118) was purchased from Amresco (Solon, OH). Reagent test kits of IL-1β, IL-18, TNF-α, IL-8, ASC, and Caspase-1 were purchased from Jianglai (Shanghai, China). The reagents for detecting MDA, GSH, SOD, and DCHF-DA were purchased from Solarbio (Beijing, China). Collagen I (sc-28654) was purchased from Santa Cruz Biotechnology (San Diego, CA, USA). The reagents for the detection of serum and fecal uric acid (UA), serum creatinine (Cre), and serum urea nitrogen (BUN) test kits were purchased from Jiancheng Biological Technology, Co., Ltd (Nanjing, China). DMSO and all other chemicals were obtained from Sigma-Aldrich (St. Louis, MO, USA).

2.2. Quails model construction

All quail surgeries were approved by the Animal Care and Ethics Committee of Beijing University of Chinese Medicine (NO. BUCM-4–2021070102–3105). Four-week-old male French quail (Beijing Deling Quail Farm) were housed in 90 × 80 × 40 cm3 cages in a temperature-controlled chamber (temperature 25 ± 2 °C, air humidity 50–55 %, and a 12-h light cycle). And the ventilation is in a standard environment. The quails were randomly divided into two groups: the control group (Con, 16 quails/group), which was fed a regular diet, and the model group (Mod, 48 quails/group), which was fed a formula supplemented with yeast and bone extract powder and drinking water containing 10 % fructose (15 mL per quail) (Patent No.202210651513.3). At 30 days of the experiment, 8 quails in Con group and Mod group were sacrificed to establish the gout quail model. The remaining quails were usually fed in the Con group. In contrast, the Mod group was randomly divided into five groups (8 quails/ group) for therapeutic administration and fed under the above conditions. Allopurinol, the treated group (All), quails were fed the same as the model group and treated with 35 mg/kg allopurinol by intragastric administration. In colchicine treated group (Col), quails were provided the same as the model group and treated with 0.6 mg/kg colchicine by intragastric administration. In the high-dosage rutin-treated group (Rut H), quails were fed the same as the model group and treated with 300 mg/kg rutin by intragastric administration. In the low-dosage rutin-treated group (Rut L), quails were fed the same as the model group and treated with 150 mg/kg rutin by intragastric administration. Feed was added twice daily, and the remainder was weighed the following day. After fasting for 12 h, cervical venous blood samples were collected. After fasting for 12 h, cervical venous blood was collected and placed at room temperature until serum precipitated. Centrifugation at 3500 r/min for 10 min, the uric acid level was detected. The joint cavity was washed with 0.2 mL normal saline, the ankle fluid was collected, and the uric acid level of the joint fluid was detected. All animals were sacrificed at the end of the experiment, and kidney and joint tissues were collected for subsequent experiments. The whole experiment lasted 40 days.

2.3. Assessment of Ankle Edema

Ankle edema formation was assessed as an increase in ankle circumference. We measured ankle circumference at 0.5 mm below the ankle joint on days 30 and 40 of the experiment. Each measurement was repeated three times, and the average value was taken. ASD is calculated using a formula [4].

Ankle swelling degree (%) = [ankle circumference after modeling (mm) - ankle circumference before modeling (mm)] / [ankle circumference before modeling (mm)] × 100 %.

2.4. Hematoxylin and eosin (HE) staining analysis of kidney and joint

Kidney and joint tissue were excised and fixed in buffered formalin (10 %). Fixed tissue specimens were used to prepare 4–6 μm thick paraffin sections, dehydrated with successive concentrations of ethanol, and then stained with H&E stain. Finally, tissue sections were observed, analyzed, and imaged using a light microscope (Leica DMR 3000; Leica Microsystems).

2.5. Measurement of biochemical indicators in Gout Quails

Blood samples and tissues were collected according to the experimental design. The serum and tissues were isolated, and SOD, MDA, GSH, XOD, TNF-α, IL-1β, IL-8, and IL-18 were detected according to the kit instructions.

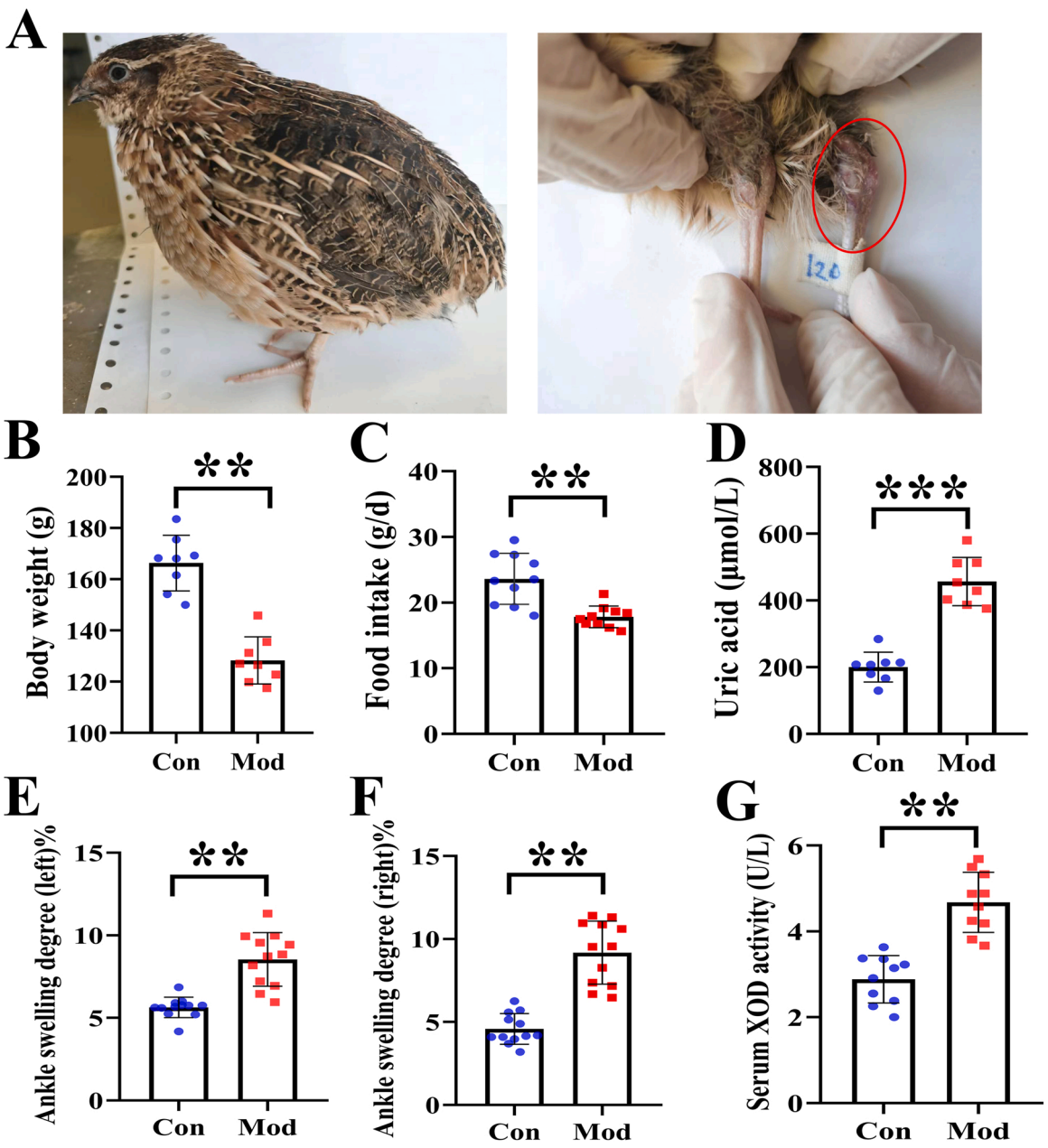

Fig. 1. The general state of quail in the modeling process. (A) Swelling degree of quail joints in Mod group. (B) The body weight of quails in each group. (C) The food intake of quail in each group. (D) The serum uric acid level in each group. The left (E) and right (F) of the swelling degree of the quail ankle joint during the experiment. (G) The XOD activity in the serum in each group. Data are expressed as mean ± SEM for 8 quails in each group. *P < 0.05, * *P < 0.01 and * **P < 0.001 versus Con group.

2.6. Acquisition and culture of primary fibroblast-like synoviocytes

In this study, fibroblast-like synoviocytes (FLS) were extracted and identified from quail for the first time. Quail bilateral posterior knee joints were cut off. After cleaning the knee joints with PBS, the quail were transferred to a PBS plate containing 100 μ/mL penicillin and 100 mg/mL streptomycin on an ultra-clean work table for synovial tissue separation. Ice bath and sterility were maintained during tissue isolation. Synovial tissue was cut into 1 mm × 1 mm× 1 mm, transferred to a 10 mL centrifuge tube, centrifuged at low speed, discarded supernatant, resuspended by adding 1 mL 0.2 % type I collagenase, transferred to culture flask, and diluted to 3 mL with collagenase to distribute synovial tissue at the bottom of culture flask evenly. The synovial cells were cultured at 37 ℃ in an incubator with 5 % CO_2 to observe the morphology and growth status of synovial cells.

2.7. Immunofluorescence staining

The number of cultured third passage synovial cells was adjusted to 5 × 104/mL and cultured for 24 h in an incubator. Add 300uL of 4 % paraformaldehyde and fix for 20 min. After permeation with 0.2 %, Triton X-100 at 37 °C for 20 min, Vimentin antibody (1:200) was added at 4 °C overnight in a wet box. Subsequently, fluorescent 488 IgG (1:500) was added at 37 °C for 1 h in the dark. After nuclei were stained with DAPI (37 °C) for 15 min, slides were fixed with an anti-fluorescence quencher. They were observed and photographed with a fluorescence microscope. The purity of FLS was determined by vimentin staining of synovial membrane cells. For example, more than 98 % of the synovial cells were stained with Vimentin, so more than 98 % of the cells were FLS.

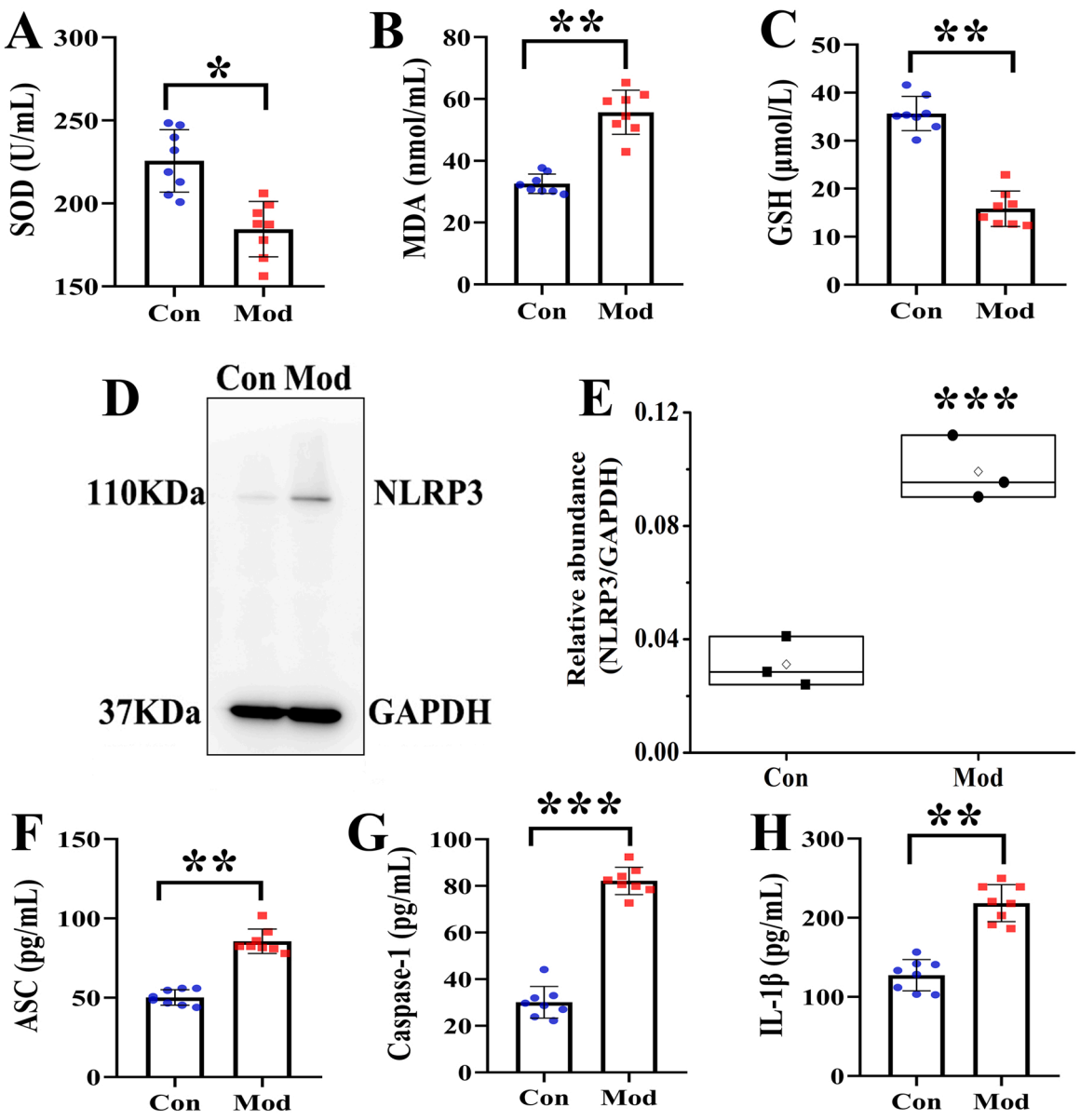

Fig. 2. The oxidative stress level and NLRP3 inflammasome was activated and IL-1β expression increased in synovial tissue. (A)The content of SOD in the joint synovial tissue. (B) The content of MDA in the joint synovial tissue. (C)The content of GSH in the joint synovial tissue. (D) Western blot was conducted to evaluate the protein level of NLRP3 and GAPDH in synovial tissue (n = 3). (E) Box plot showing the densitometry analysis of NLRP3 normalized by GAPDH. (F) The expression level of ASC in synovial tissue. (G) The expression level of Caspase-1 in synovial tissue. (H) The expression level of IL-1β in synovial tissue. Data are expressed as mean ± SEM for 8 quails in each group. *P < 0.05, * *P < 0.01 and * **P < 0.001 versus Con group.

2.8. Cell treatment

FLS were cultured in DMEM containing 10 % fetal bovine serum (Gibco), 100 U/mL penicillin, and 100 U/mL streptomycin at 37∘C in a wet incubator containing 5 % CO2. Then uric acid (UA, 600 μM) was added to the model group, and rutin (Rut, 50 μM) was added to the treatment group for 24 h. Twenty-four hours after stimulation, cells were harvested for further analysis. All in vitro experiments were repeated no less than three times.

2.9. Immunoblot Analysis

Synovial tissue samples were removed and homogenized with cell lysis buffer, PMSF, and phosphatase inhibitors. FLS were washed three times with ice-cold PBS and collected in RIPA buffer containing PMSF and phosphatase inhibitors. Proteins were separated by SDS-PAGE and transferred to 0.2 mM nitrocellulose membranes. After incubation with 5 % skims milk for 1 h at room temperature, cells were incubated with primary antibody overnight at 4 °C, followed by incubation with the appropriate amount of horseradish peroxidase-conjugated secondary antibody for 1 h at room temperature. Bound antibodies are detected by chemiluminescence. Image J software (National Institutes of Health, Bethesda, MD) was used to analyze the optical density of the immunoblot results.

2.10. Statistical analysis

Data are presented in the figure as mean ± SEM for each group. All results were tested for normality to determine the use of parametric or nonparametric tests. Data containing two normally distributed groups were analyzed with the unpaired student t-test and with the Mann-Whitney U test for nonparametric data. When more than two factors

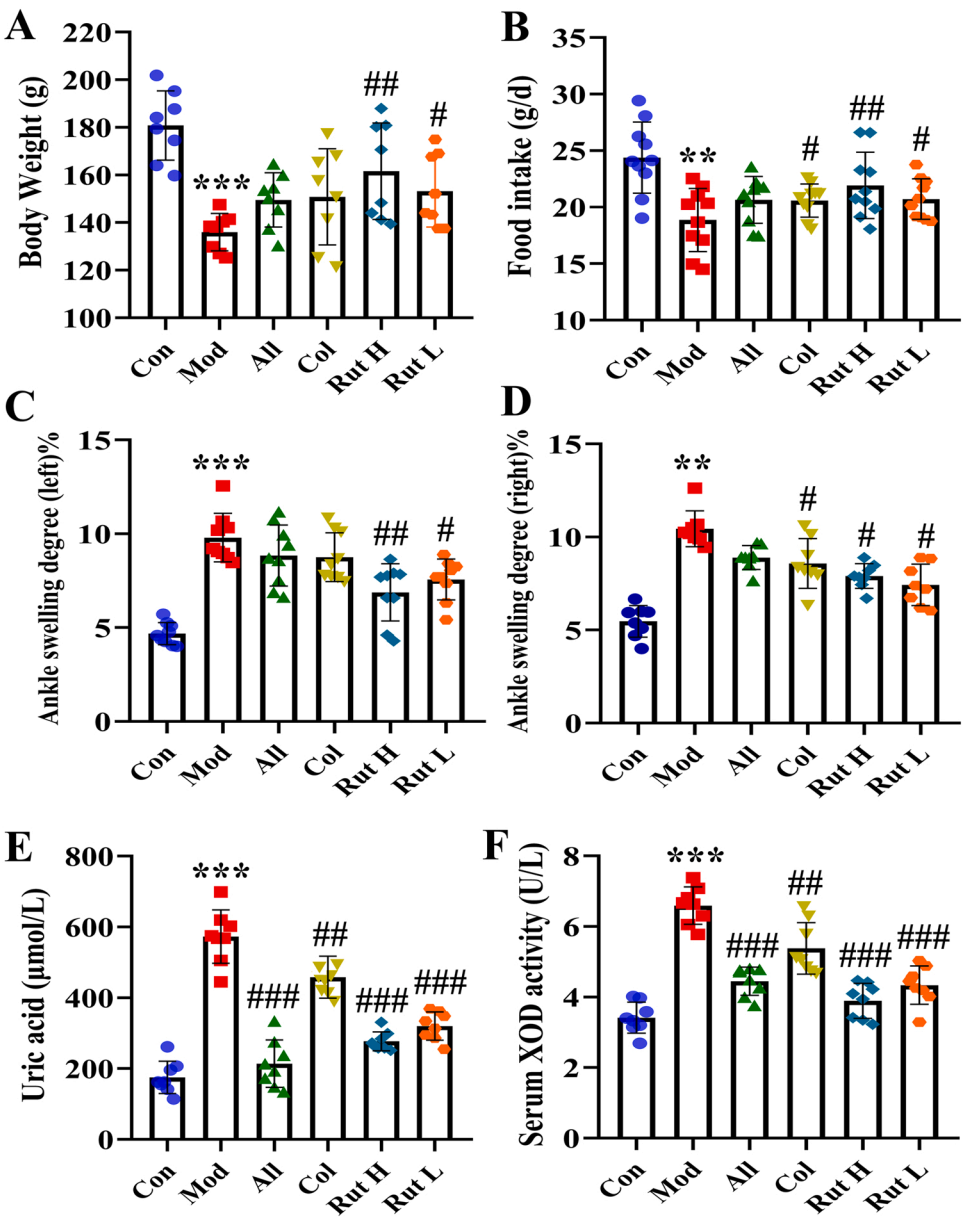

Fig. 3. The general state of quail after rutin treatment. (A) The body weight of quails in each group. (B) The food intake of quail in each group. The left (C) and right (D) of the swelling degree of the quail ankle joint after treatment. (E) The serum uric acid level in each group. (F) The XOD activity in the serum in each group. Data are expressed as mean ± SEM for 8 quails in each group. *P < 0.05, * *P < 0.01 and * **P < 0.001 versus Con group, #P < 0.05, ##P < 0.01 and ###P < 0.001 versus Mod group.

were present in the analysis, a two-way ANOVA test was performed, followed by Sidak's multiple comparison test. Statistically significant differences between means are marked in each graph. P < 0.05 was considered statistically significant.

3. Results

3.1. General state and expression level of uric acid of quail after modeling

In this study, the quails in the Con group were in a normal mental state, with shiny feathers, loud calls, and lively and active; the quails in the Mod group were in a poor mental state, with black feathers, low calls, and less activity. In addition, the quail joints in the Mod group were significantly swollen, which was consistent with the clinical features of gout (Fig. 1-A). Compared with the Con group, the body weight level of the quails in the Mod group was significantly lower in the experiment (P < 0.01) (Fig. 1-B). The food intake of the quails in the Mod group was significantly decreased (P < 0.01) (Fig. 1-C). And the ankle swelling in the Mod group was significantly increased (P < 0.01) (Fig. 1-EF), indicating that the quails in the Mod group developed gout symptoms. The uric acid levels of quails in each group at 30 days were detected. The results showed that compared with the Con group, the serum uric acid levels of the quails in the Mod group were significantly increased (P < 0.001) (Fig. 1-D), and the expression level of XOD was also increased considerably (P < 0.01) (Fig. 1-G). This part showed that 30 days after modeling, the quails in the Mod group developed obvious gout symptoms, and the serum uric acid level and uric acid-producing enzyme were significantly increased.

3.2. Expression levels of oxidative stress and NLRP3 inflammasome after modeling

On the 30th day of the experiment, eight quails in each group were sacrificed, and cervical venous blood and synovial tissue were collected. The levels of oxidative stress in quail in each group were detected. The results showed that SOD content in the synovium of the joint of quail in the Mod group was significantly lower than in the Con group (P < 0.05). MDA content in the Mod group was significantly higher than in the Con group (P < 0.01). And GSH content in the MOD group was significantly lower than in the Con group (P < 0.01). These results suggested that the

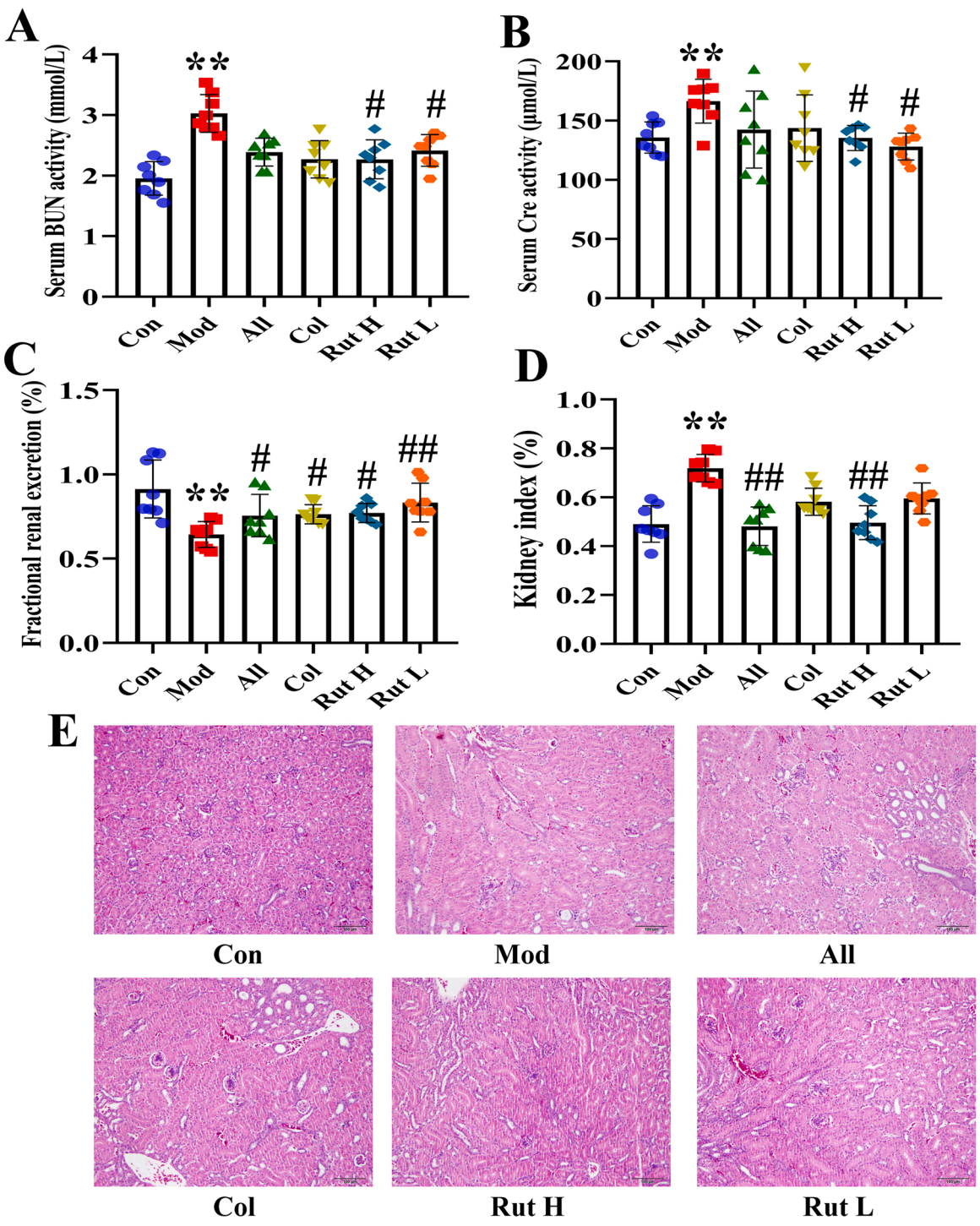

Fig. 4. Serum kidney function, HE staining of quails in different groups. (A)The activity of Bun in the serum. (B) The activity of Cre in the serum. (C) The fractional renal uric acid excretion of the quails. (D) Kidney index. (E) HE staining. *P < 0.05, * *P < 0.01 and * **P < 0.001 versus Con group, $^{\#}$P < 0.05, $^{\#\#}$P < 0.01 and $^{\#\#\#}$P < 0.001 versus Mod group.

oxidative stress level in the model quail was destroyed 30 days after modeling (Fig. 2-ABC). We also detected the expression of NLRP3, ASC, Caspase-1, and IL-1β in synovial tissue. The results showed that the expression of NLRP3 in the Mod group was significantly higher than in the Con group at 30 days. After performing Image J analysis, NLRP3 expression was significantly increased in the Mod group compared to the Con group (P < 0.001) (Fig. 2-DE). The expression levels of ASC, Caspase-1, and IL-1β in synovial tissue of quail in each group were analyzed. On the 30th day of the experiment, the expression level of ASC in the Mod group was significantly higher than that in the Con group (P < 0.01) (Fig. 2-F). The expression level of Caspase-1 was detected, and the expression of the Mod group was significantly higher than that of the Con group (P < 0.001) (Fig. 2-G). Finally, the expression of IL-1β in synovial tissue of quail joints was detected, and the results showed that the expression level of IL-1β in the Mod group was significantly higher than that in the Con group at 30 days of the experiment (P < 0.01) (Fig. 2-H).

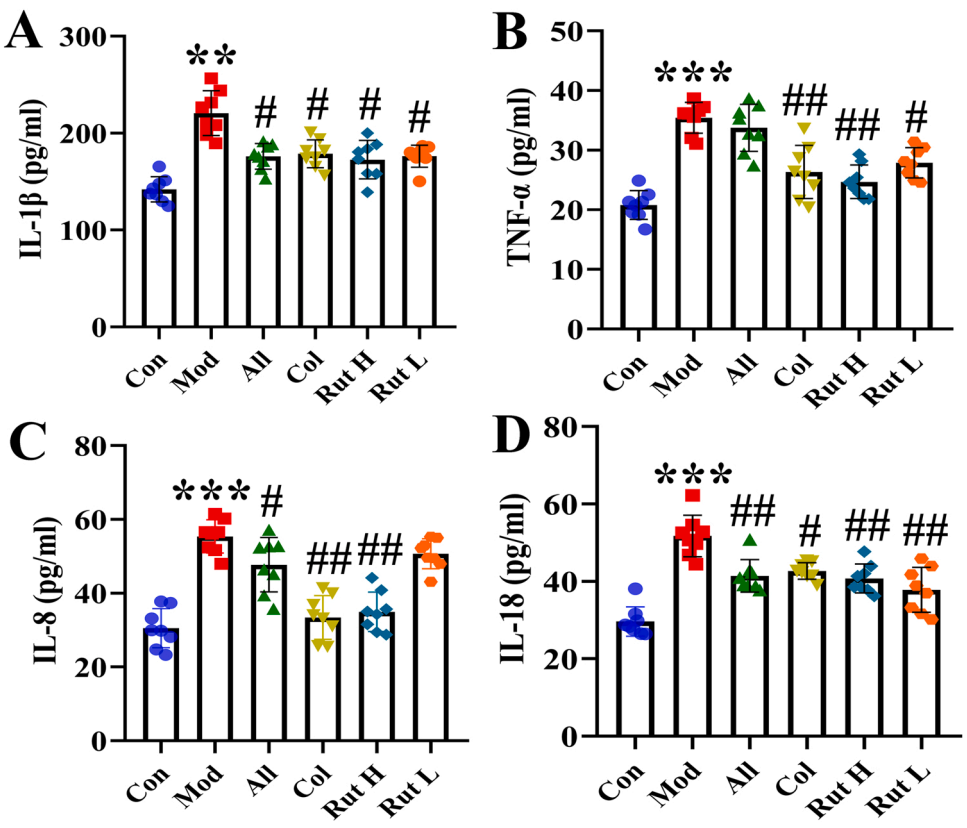

Fig. 5. Expression of inflammatory factors in the serum of quails in each group. (A) The expression levels of IL-1β in the serum. (B) The expression levels of TNF-α in the serum. (C) The expression levels of IL-8 in the serum. (D) The expression levels of IL-18 in the serum. Data are expressed as mean ± SEM for 8 quails in each group. *$P < 0.05$, * *$P < 0.01$ and * **$P < 0.001$ versus Con group, $^{\#}P < 0.05$, $^{\#\#}P < 0.01$ and $^{\#\#\#}P < 0.001$ versus Mod group.

3.3. General state and expression levels of uric acid of quail after rutin treatment

After 30 days of the experiment, the quails in each group were treated with drugs, and the general state and uric acid levels were observed. The results showed that the body weight of the quail in the Mod group was significantly decreased compared with the Con group ($P < 0.001$). In contrast, the body weight of quail in the Rut H and Rut L groups was significantly increased compared with the Mod group ($P < 0.05$ or $P < 0.01$) (Fig. 3-A). The food intake of quail in the Mod group was significantly decreased compared with that in the Con group ($P < 0.01$), and the food intake of quail in Col, Rut H, and Rut L groups was significantly increased compared with that in Mod group ($P < 0.05$ or $P < 0.01$) (Fig. 3-B). Ankle swelling was significantly increased in the Mod group ($P < 0.01$), indicating gout symptoms in quail in the Mod group, and rutin treatment could effectively reduce ankle swelling ($P < 0.05$ or $P < 0.01$) (Fig. 3-CD). The levels of uric acid and XOD expression in the serum of quail in each group were detected. Compared with the Con group, the levels of uric acid and XOD expression in the Mod group were significantly increased ($P < 0.001$). The expression levels of uric acid and XOD of quail in Rut H and Rut L groups were significantly lower than those in the Mod group ($P < 0.001$) (Fig. 3-EF). The results showed that rutin treatment could effectively alleviate the gout symptoms of quail in the Mod group and reduce the expression levels of serum uric acid and uric acid-producing enzymes.

3.4. Renal function level and staining of HE

To investigate the effect of rutin treatment on the renal function of quail. Compared with the Con group, the serum urea nitrogen level of quail in the Mod group was significantly increased ($P < 0.01$). In contrast, the serum urea nitrogen level of quail in the Rut H and Col groups was significantly decreased compared with the Mod group ($P < 0.05$) (Fig. 4-A). The serum creatinine level of the quail in the Mod group was significantly increased compared with the Con group ($P < 0.01$), and the creatinine level of quail in the Rut H and Rut L groups was significantly decreased compared with the Mod group ($P < 0.05$) (Fig. 4-B). The renal excretion fraction and renal index of quail in each group were detected. Compared with the Con group, the renal excretion fraction of quail in the Mod group was significantly decreased ($P < 0.01$), and the renal index was significantly increased ($P < 0.01$). Compared with the Mod group, the renal excretion fraction of quail in Rut H and Rut L groups was significantly increased ($P < 0.05$ or $P < 0.01$), and the renal index was significantly decreased ($P < 0.01$) (Fig. 4-CD). HE staining showed that the renal structure of the quail in the Con group was normal, the renal tissue of the quail in the Mod group showed a large number of glomerular atrophy, renal tubule dilatation, epithelial cell necrosis, and shedding, and the renal tissue of quail in Rut H, Rut L, and Col groups showed vacuolar degeneration of some renal tubules. Renal tissue of some quail in the All group showed glomerular atrophy, renal tubule lumen dilation, and cell boundary disorder (Fig. 4-E). The results showed that the renal function and structure of quails in the Mod group were damaged, which could be relieved by rutin treatment.

3.5. Cytokine expression levels

ELISA kits detected the changes in IL-1β, IL-18, TNF-α, and IL-8 cytokines. The results showed that compared with the Con group, the expression levels of IL-1β, IL-18, TNF-α, and IL-8 cytokines in the Mod group were significantly increased ($P < 0.01$ or $P < 0.001$). Compared with the Mod group, the expression levels of IL-1β, IL-18, TNF-α, and IL-8 in the Rut H group were significantly decreased ($P < 0.05$ or $P < 0.01$). The expression levels of IL-1β, IL-18, and TNF-α cytokines in

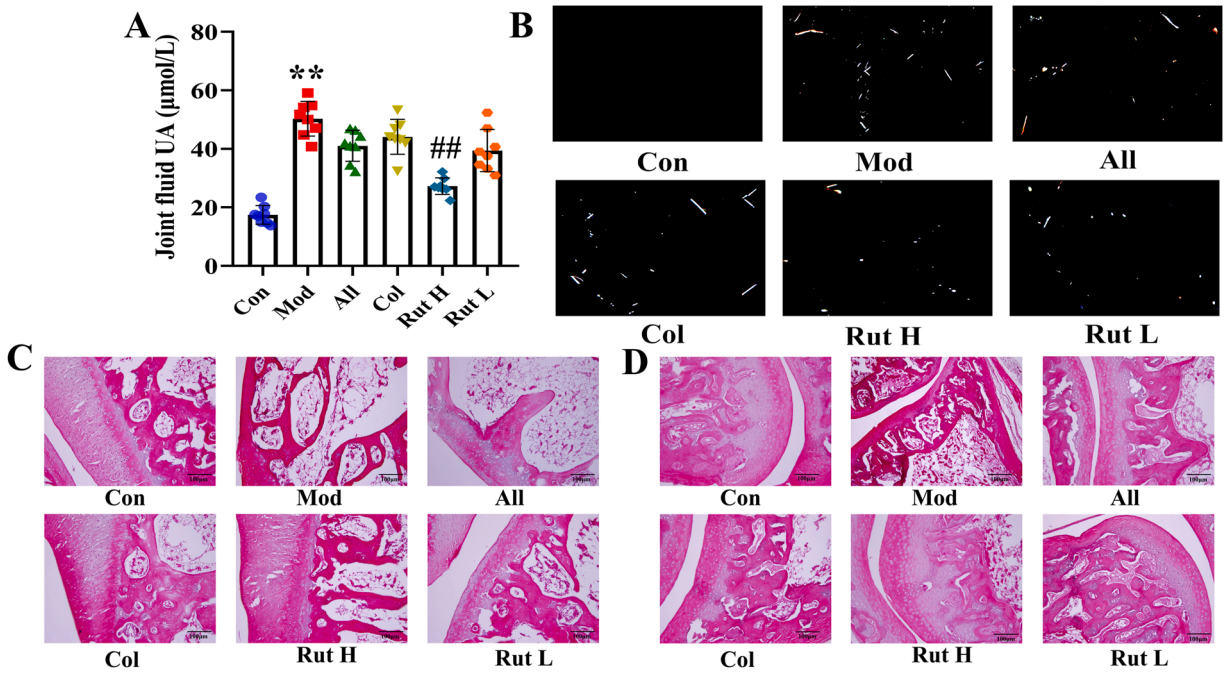

Fig. 6. The levels of uric acid in joint fluid and HE staining of joints of quails in each group after rutin treatment. (A) The joint fluid uric acid level of the quails. (B) The urate crystals appeared in the synovial fluid of quails. (C) HE staining of ankle joint (200 ×). (D) HE staining of claw joint (200 ×). Data are expressed as mean ± SEM for 8 quails in each group. *P < 0.05, * *P < 0.01 and * **P < 0.001 versus Con group, $^{\#}$P < 0.05, $^{\#\#}$P < 0.01 and $^{\#\#\#}$P < 0.001 versus Mod group.

quail in the Rut L group were significantly decreased (P < 0.05 or P < 0.01) (Fig. 5). The results showed an inflammatory response in the quail in the Mod group, and rutin treatment could reduce the expression of proinflammatory factors in the quail.

3.6. The effect of rutin treatment for uric acid level in synovial fluid, polarized light observation, and HE staining

We detected the level of uric acid in the joint fluid of quail in each

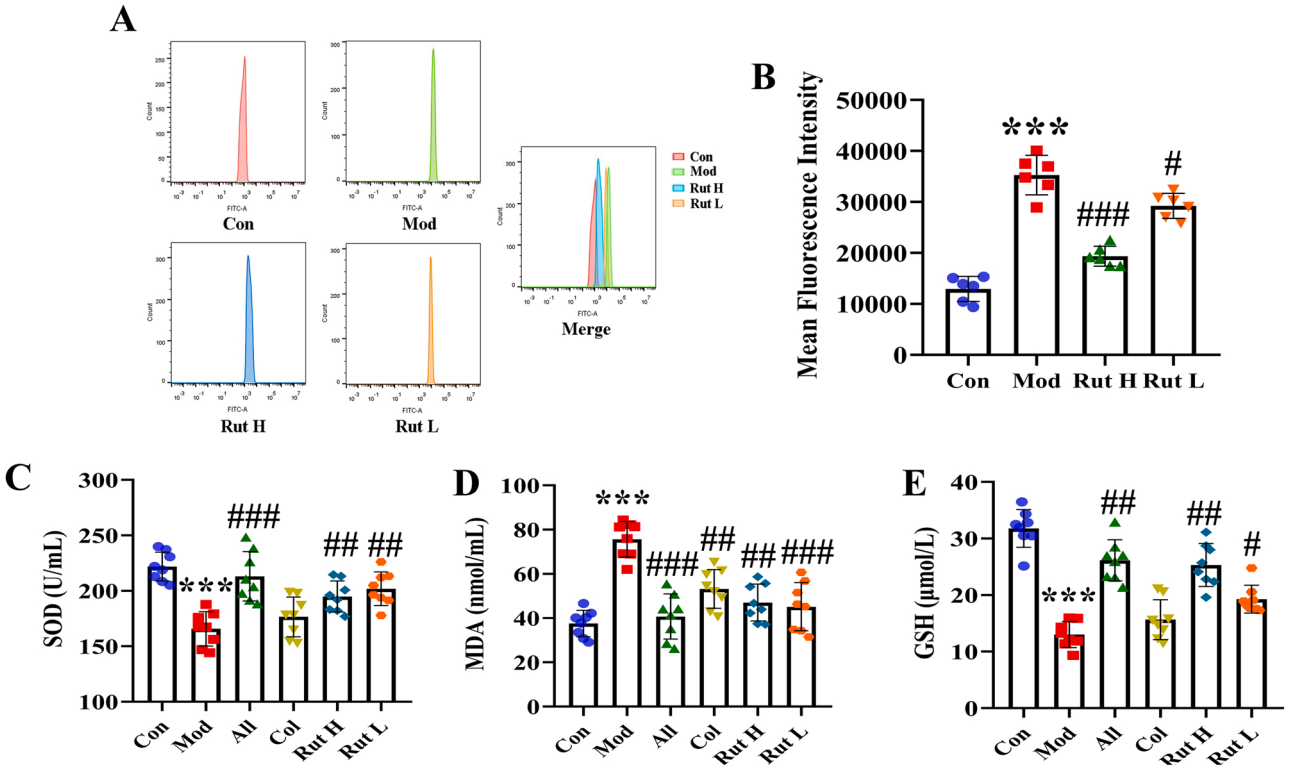

Fig. 7. The level of oxidative stress in the joint synovial tissue of quails after rutin treatment. (A) Detection of ROS expression levels in the joint synovial tissue by flow cytometry. (B) The mean fluorescence intensity of the joint synovial tissue in each group. (C)The content of SOD in the joint synovial tissue. (D) The content of MDA in the joint synovial tissue. (E)The content of GSH in the joint synovial tissue. Data are expressed as mean ± SEM for 8 quails in each group. *P < 0.05, * *P < 0.01 and * **P < 0.001 versus Con group, $^{\#}$P < 0.05, $^{\#\#}$P < 0.01 and $^{\#\#\#}$P < 0.001 versus Mod group.

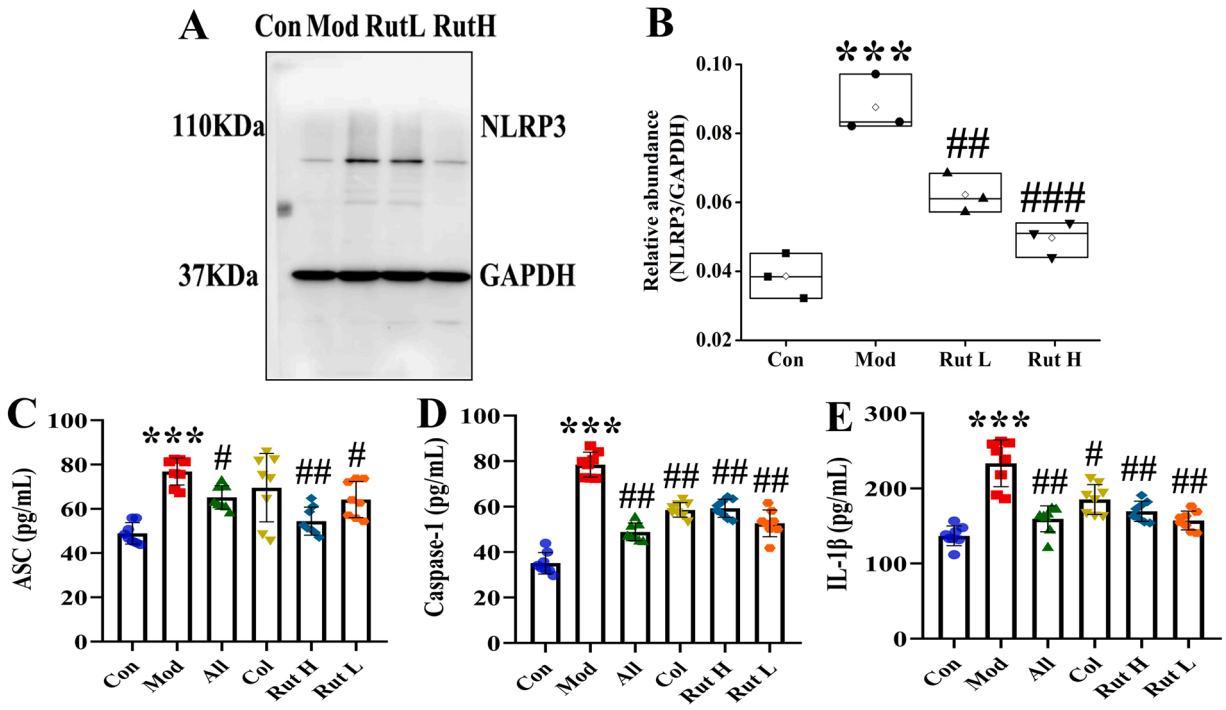

Fig. 8. Rutin alleviates NLRP3 inflammasome in gouty quail. (A) Western blot was conducted to evaluate the protein level of NLRP3 and GAPDH in synovial tissue. (B) Box plot showing the densitometry analysis of NLRP3 normalized by GAPDH. (C) The expression level of ASC in synovial tissue. (D) The expression level of Caspase-1 in synovial tissue. (E) The expression level of IL-1β in synovial tissue. Data are expressed as mean ± SEM for 8 quails in each group. *P < 0.05, * *P < 0.01 and * **P < 0.001 versus Con group, $^{\#}$P < 0.05, $^{\#\#}$P < 0.01 and $^{\#\#\#}$P < 0.001 versus Mod group.

group, and the results showed that the level of uric acid in the joint fluid of quail in the Mod group was significantly higher than that in the Con group (P < 0.01), and the level of uric acid in the Rut H group was significantly lower than that in the Mod group (P < 0.01) (Fig. 6-A). The joint fluid of quail was observed under a polarized light microscope at 200 times. Under the black field, no urate crystals were observed in the Con group. Compared with the Con group, blue-yellow bright, needle or fine rod-shaped urate crystals were observed in the model group, and a few crystals were observed in the Rut H group compared with the Mod group (Fig. 6-B). The HE staining of quail ankle tissue showed that the quail ankle tissue structure in Con group was clear, the joint surface was smooth and flat, and the synovial cells were loose and normal in shape. Synovial fibrous tissue hyperplasia, pannus formation and a large number of inflammatory cells infiltration were observed in the ankle tissues of Mod group. Compared with the Mod group, the inflammatory cell infiltration and the degree of synovial fibrous tissue proliferation were significantly reduced in the Rut H, Rut L and Col groups. In the Con group, the paw joint tissue structure was clear, the joint surface was smooth, and the synovial tissue morphology was normal. In the Mod group, obvious cartilage and bone destruction, synovial fibrous tissue proliferation, and inflammatory cell infiltration were observed in the paw joint tissue of quail. Compared with the Mod group, there was a small amount of inflammatory cell infiltration in the Rut H and Rut L groups, which could alleviate synovial fibrous tissue hyperplasia to different degrees (Fig. 6-CD).

3.7. Oxidative stress levels after rutin treatment

The levels of oxidative stress in synovial tissues of quail joints were measured. Flow cytometry was used to detect ROS expression in each group's joint synovial tissue. The experimental results showed that compared with the Con group, the ROS fluorescence intensity of the Mod group was significantly increased (P < 0.001). The fluorescence intensity of Rut H and Rut L groups was significantly decreased than that of Mod group (P < 0.05 or P < 0.001) (Fig. 7-AB). The results showed that compared with the Con group, the SOD content in the joint synovial tissue of quail in the Mod group was significantly lower than that in the Con group (P < 0.001). And the SOD content in the body of quail in the Rut H and Rut L groups was significantly higher than that in the Mod group (P < 0.01) (Fig. 7-C). The level of MDA in synovial tissue of quail in the Mod group was significantly increased compared with that in the Con group (P < 0.001), and the level of MDA in Rut H and Rut L groups was significantly decreased compared with that in Mod group (P < 0.01 or P < 0.001) (Fig. 7-D). We further detected the expression level of GSH in synovial tissues, and we found that compared with the Con group, the content of GSH in synovial tissues of quail joints in the Mod group was significantly lower than that in the Con group (P < 0.001). The GSH content in quail in Rut H and Rut L groups was significantly increased compared with that in the Mod group (P < 0.05 or P < 0.01) (Fig. 7-E).

3.8. Expression levels of NLRP3 inflammasome after rutin treatment

We detected the expression of NLRP3, ASC, Caspase-1, and IL-1β in each group's synovial tissue of quail. The results showed that the expression of NLRP3 in the Mod group was significantly higher than that in the Con group at 40 days of the experiment. After analysis, the expression of NLRP3 in the Mod group was significantly increased compared with that in the Con group (P < 0.001). And the expression of NLRP3 in the Rut H and Rut L group was significantly decreased compared with the Mod group (P < 0.01 or P < 0.001) (Fig. 8-AB). The expression levels of ASC, Caspase-1, and IL-1β in synovial tissue of quail in each group were analyzed. On the 40th day of the experiment, the expression level of ASC in the Mod group was significantly higher than that in the Con group (P < 0.001), and the expression level of ASC in the Rut H and Rut L groups was significantly lower than the Mod group (P < 0.05 or P < 0.01) (Fig. 8-C). The expression level of Caspase-1 in the Mod group was significantly higher than the Con group (P < 0.001), and the expression level of quail in the Rut H and Rut L groups was significantly decreased (P < 0.01) (Fig. 8-D). Finally, the expression of IL-1β in the synovial tissue of quail joints was detected. The results

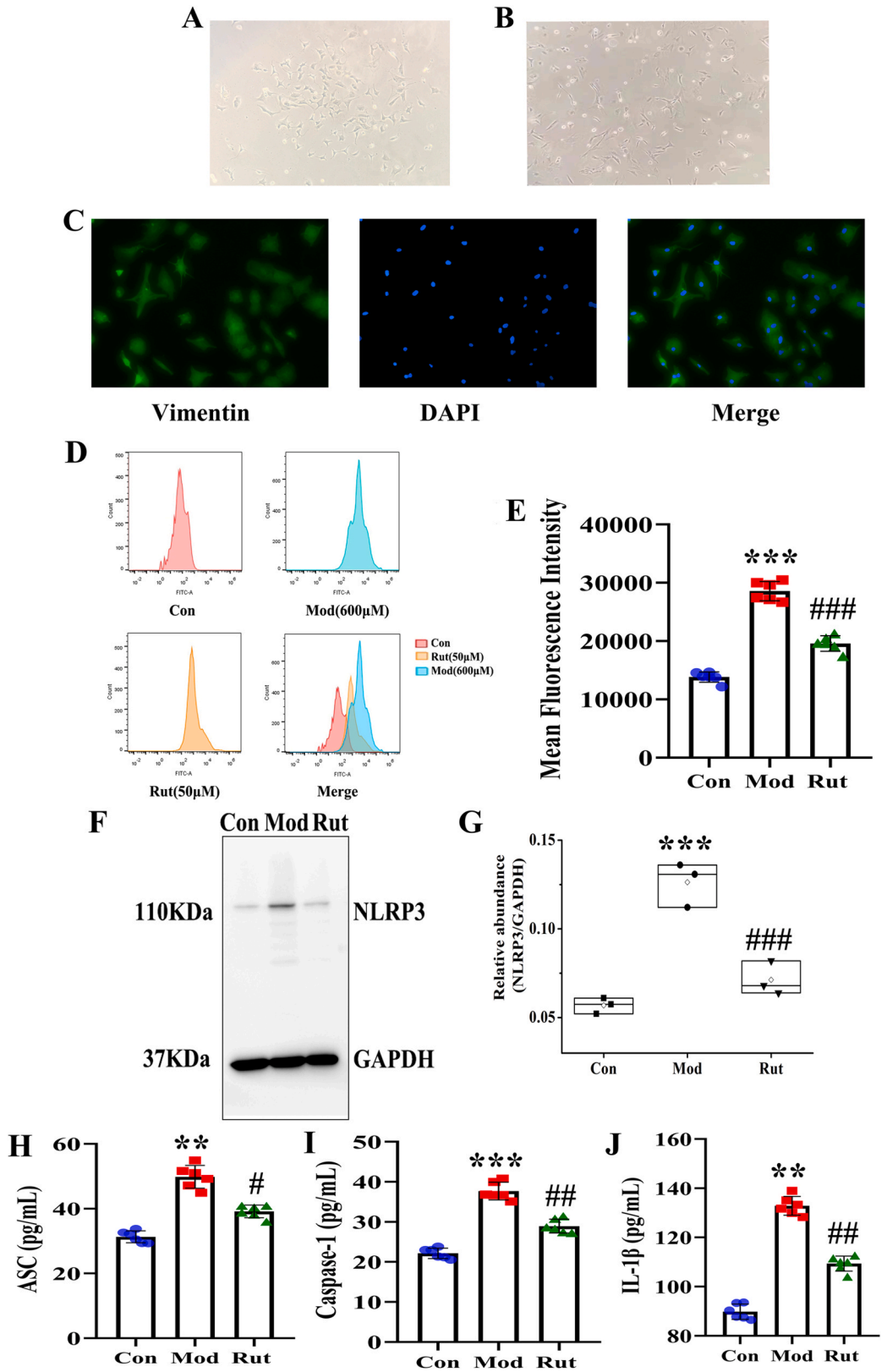

Fig. 9. Extraction and identification of FLS and rutin inhibits ROS and NLRP3 inflammasome in FLS after uric acid stimulation. (A) Morphology of the first generation FLS. (B) Morphology of the third-generation FLS. (C) Vimentin identifies FLS as a characteristic labeling protein. (D) Detection of ROS expression levels in FLS after adding uric acid and rutin treatment by flow cytometry. (E) The mean fluorescence intensity of FLS in each group. (F) Western blot was conducted to evaluate the protein level of NLRP3 and GAPDH in cell lysates. (G) Box plot showing the densitometry analysis of NLRP3 normalized by GAPDH. (H) The expression level of ASC in cell supernatant. (I) The expression level of Caspase-1 in cell supernatant. (J) The expression level of IL-1β in cell supernatant. *$P < 0.05$, * *$P < 0.01$ and * **$P < 0.001$ versus Con group, $^{\#}P < 0.05$, $^{\#\#}P < 0.01$ and $^{\#\#\#}P < 0.001$ versus Mod group.

showed that the expression level of IL-1β in the Mod group was significantly higher than the Con group ($P < 0.001$). In contrast, the expression level of IL-1β in the synovial tissue of quail in the Rut H and Rut L groups was significantly lower ($P < 0.01$) (Fig. 8-E). These results indicated that rutin treatment could inhibit the activation of NLRP3 inflammasome and exert anti-NLRP3 effects.

3.9. Effects of ROS and NLRP3 inflammasome in FLS after rutin treatment

Synovial tissue from quail joints was isolated for cell culture. After one day of culture, the cells swam out. Most of them were spindle-shaped (Fig. 9-A). On the 10th day of culture, the synovial cells of the third generation showed spindle shape. The cells grew and proliferated well (Fig. 9-B). Immunostaining showed that the cell morphology was regular and spindle-shaped, and the nucleus was oval in the center of the cell. Vimentin is a characteristic marker protein of FLS, suggesting that the cultured synovial cells are FLS, and the positive rate of vimentin staining in synovial cells is more than 98 % (Fig. 9-C).

To explore the effect of rutin on ROS and NLRP3 inflammasome in FLS. According to the results of previous research and cell viability experiments of our research group, 50 μM rutin was selected as the experimental drug group for analysis. The Mod group was stimulated with 600 μM uric acid, the Rut group, was stimulated with uric acid, and 50 μM rutin was added for observation. After 24 h, the expression of ROS in the cell supernatant was detected by flow cytometry. Compared with other groups, the fluorescence intensity of ROS in the Mod group was significantly increased ($P < 0.001$). In contrast, the fluorescence intensity of ROS in the Rut group was significantly lower than that in the Mod group ($P < 0.001$), indicating that uric acid stimulation increased the expression of ROS in the FLS. Rutin could reduce the over-expression of ROS caused by uric acid (Fig. 9-DE).

The expressions of NLRP3, ASC, Caspase-1, and IL-1β in cell lysates of each group were detected. The results showed that the expression level of NLRP3 in the Mod group was significantly higher than in the Con group ($P < 0.001$). The expression level of NLRP3 protein in the Rut group was significantly lower than that in the Mod group ($P < 0.001$) (Fig. 9-FG). At the same time, the expression levels of ASC, Caspase-1, and IL-1β in the Mod group were significantly higher than those in the Con group ($P < 0.01$ or $P < 0.001$). In contrast, the expression levels of ASC, Caspase-1, and IL-1β in the Rut group were significantly lower than those in the Mod group ($P < 0.05$ or $P < 0.01$) (Fig. 9-HIJ).

4. Discussion

Gout is a progressive metabolic disease closely related to hyperuricemia and urate deposition. The pathogenesis of gout includes hyperuricemia, MSU crystalline deposition, and acute inflammation, characterized by progressive and recurrent disease [7,8]. Gout is caused by abnormally elevated circulating urate levels, resulting in urate crystals in joints, tendons, and other tissues [5,43]. Recent studies have shown a high incidence of gout worldwide, including among young people [4,5]. Gout can cause considerable disability, health loss, and economic burden, and there is an urgent need for clinical treatment [6]. In 2019, the Gout, Hyperuricemia, and Crystal-Associated Diseases Network (G-CAN) defined hyperuricemia and gout as different states of the same disease [44]. It can be seen that the latest studies have a new understanding of the development characteristics of gout as a whole and gradually realize that asymptomatic hyperuricemia and gout are a continuous pathological process. At the same time, improving the sensitivity and specificity of glycoprotein in clinical detection of gout can also provide reference for further research on gout [11].

In the study of gouty animal models, we found that many scholars adopted the method of Coderre et al. to establish gouty arthritis animal models by local injection of sodium urate into joints [45]. In the gout model constructed by MSU injection, only local inflammatory reactions could be observed, including knee joint injection, foot pad injection, ankle joint injection, etc. This modeling method has a short duration and low specificity. Our research group has been studying gout-related animal models for a long time and finally adopted quail as the model animal, which has a similar metabolic pathway of uric acid to humans [38–42]. Quail do not contain urate oxidase, which is physiologically consistent with human uric acid metabolism. The modeling method used in this study simulated the whole pathological process from hyperuricemia to gout attack in clinical practice, and the gout model was more in line with the characteristics of human uric acid metabolism. In addition, the induction method simulates the clinical high-purine diet, which is consistent with the clinical etiology of gout and is an advantageous animal model for developing gout prevention and treatment drugs.

The formation of hyperuricemia is related to abnormal uric acid homeostasis in vivo, and its pathological process is closely related to the target groups of uric acid metabolism [46,47]. Uric acid is the end

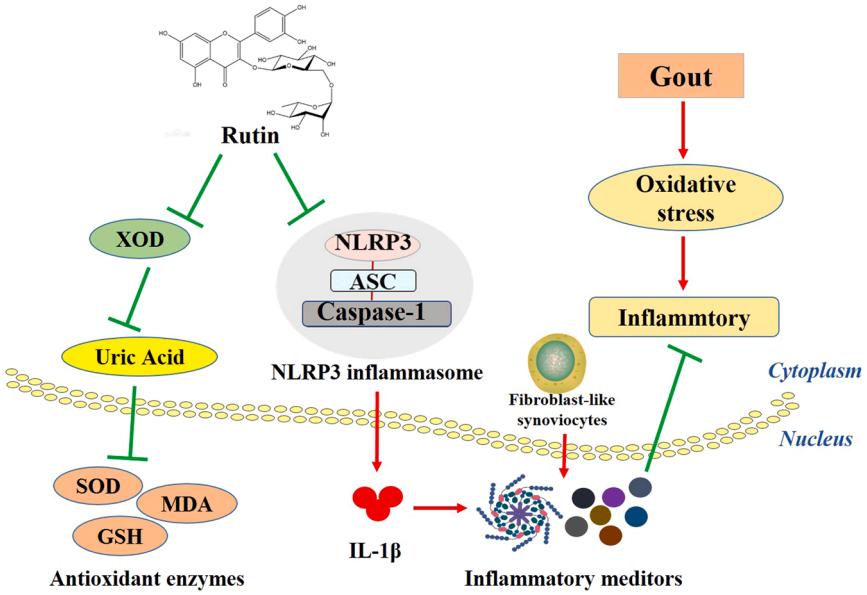

Fig. 10. Schematic model of the inhibitory effect of rutin on gout. Rutin ameliorates gout via inhibiting XOD activity, ROS and NLRP3 inflammasome activation.

product of purine metabolism in the human body, and the physiological concentration of uric acid is an essential antioxidant for the human body, which can reduce oxidative damage caused by ROS. Uric acid beyond the physiological concentration is mainly deposited in the form of crystals in human tissues or organs, which is considered a danger signal that can induce mitochondrial damage, promote the release of ROS expression, activate signaling pathways such as the NLRP3 inflammasome, and cause tissue and organ damage. Therefore, new therapeutic strategies for gout must consider modulating uric acid metabolic targets and inflammation production.

Rutin is a natural flavonoid derivative with a wide range of pharmacological effects, including myocardial protective [12–16], anti-inflammatory [17–19], antioxidant [20–24], anti-apoptosis [25–27], and other effects [28–32]. We have conducted many literature searches on the dosage of rutin in pharmacological experiments. The results show that rutin has good pharmacological activity at 50 mg/kg-300 mg/kg in rats or mice [48–54]. Therefore, before the formal experiment, we conducted a preliminary experimental study on the dosage of rutin on quail models. Our results showed that 300 mg/kg rutin dose did not affect quail's body weight, food intake, and other general states. At the same time, the indexes of liver and kidney function were detected 10 days after the administration of rutin, and the liver and kidney were histopathologically observed. And we tested the liver function and kidney function index after 10 days of rutin administration. The results showed that compared with the Con group, this dose of rutin did not affect the liver function and kidney function of quail ($P > 0.05$). Histopathological results showed that after 300 mg/kg rutin administration, liver and kidney tissue structure was normal, epithelial cells were arranged neatly, and no inflammatory infiltration and pathological changes were observed in quail (Fig. S1).

Gout is a metabolic disease closely related to the target of uric acid metabolism and inflammation. Rutin has anti-inflammatory effect, but the protective effect of rutin on gout has not been elucidated. Therefore, the quail gout model induced by a high-purine diet was used to conduct experiments in this study. And it was clear that quail had gout symptoms at 30 days of the experiment, and the expression of XOD in vivo was increased, the level of uric acid was increased, the balance of oxidative stress was destroyed, the NLRP3 inflammasome was activated, and inflammatory response was generated. After treatment with rutin, it can effectively relieve the symptoms of gout in quail and reduce the level of uric acid and inflammation in the body. Further study on the mechanism of action showed that rutin could reduce the level of uric acid in vivo by inhibiting the activity of XOD, restore the balance of oxidative stress by reducing the level of ROS, inhibit the activation of the NLRP3 inflammasome, and reduce the expression of inflammatory factors (Fig. 10). This study further demonstrates the potential of rutin as a gout drug.

5. Conclusion

In conclusion, our data show that rutin attenuates gout by reducing XOD activity, inhibiting ROS production and NLRP3 inflammasome activation. Our findings underscore rutin as a promising agent for the treatment of gout.

Funding

The study received funding from the National Natural Science Foundation of China (grant number U20A20406, 82104475); the Beijing Municipal Natural Science Foundation (grant number 7212178).

CRediT authorship contribution statement

BZ and ZL conceived the study. HW wrote the manuscript. YW, YL, and JH reviewed and revised the manuscript. All authors contributed to manuscript revision, read, and approved the submitted version.

Conflict of interest statement

The authors have declared no conflicting interests.

Data Availability

Data will be made available on request.

Appendix A. Supporting information

Supplementary data associated with this article can be found in the online version at doi:10.1016/j.biopha.2022.114175.

References

[1] M.C. Fisher, S.K. Rai, N. Lu, Y. Zhang, H.K. Choi, The unclosing premature mortality gap in gout: a general population-based study, Ann. Rheum. Dis. 76 (2017) 1289–1294.
[2] S.K. Rai, J.A. Aviña-Zubieta, N. McCormick, M.A. De Vera, K. Shojania, E.C. Sayre, H.K. Choi, The rising prevalence and incidence of gout in British Columbia, in: Semin Arthritis Rheum, 46, Population-based trends from 2000 to 2012, Canada, 2017, pp. 451–456.
[3] M. Kumar, N. Manley, T.R. Mikuls, Gout flare burden, diagnosis, and management: navigating care in older patients with comorbidity, Drugs Aging 38 (2021) 545–547.
[4] F. Perez-Ruiz, N. Dalbeth, T. Bardin, A review of uric acid, crystal deposition disease, and gout, Adv. Ther. 32 (2015) 31–41.
[5] S.K. Rai, L.C. Burns, M.A. De Vera, A. Haji, D. Giustini, H.K. Choi, The economic burden of gout: a systematic review, Arthritis Rheum. 45 (2015) 75–80.
[6] B.T. Burke, A. Köttgen, A. Law, B.G. Windham, D. Segev, A.N. Baer, J. Coresh, M. A. McAdams-DeMarco, Physical function, hyperuricemia, and gout in older adults, Arthritis Care Res. 67 (2015) 1730–1738.
[7] N. Dalbeth, T.R. Merriman, L.K. Stamp, Gout, Lancet 388 (10055) (2016) 2039–2052.
[8] Dalbeth Nicola, L.Gosling Anna, Gaffo Angelo, Abhishek Abhishek, Gout, Lancet 397 (2021) 1843–1855, https://doi.org/10.1016/S0140-6736(21)00569-9.
[9] Morelli J. Gout Treatment Guidelines by the American College of Rheumatology [EB/OL].[2019-11–13].⟨https://www.arthritis.org/diseases/more-about/⟩gout-treatment-guidelines.
[10] A. Qaseem, R.P. Harris, M.A. Forciea, Management of acute and recurrent gout: a clinical practice guideline from the american college of physicians, Ann. Intern. Med. 166 (01) (2017) 58–68.
[11] B. Gga, L.C. Chen, D. Wf, et al., Brilliant glycans and glycosylation: Seq and ye shall find, Int. J. Biol. Macromol. 189 (2021) 279–291.
[12] Ozbek Topali, A. Bilgin, F. Keskin, et al., The effect of rutin on cisplatin-induced oxidative cardiac damage in rats, Anatol. J. Cardiol. 20 (3) (2018) 136–142.
[13] X. Liu, L. Zheng, M. Liu, Protective effects of rutin on lipopolysaccharide-induced heart injury in mice, J. Toxicol. Sci. 43 (5) (2018) 329–337.
[14] Q. Li, M. Qin, T. Lit, Rutin protects against pirarubicin-induced cardiotoxicity by adjusting microRNA-125b-1-3p-mediated JunD signaling pathway, Mol. Cell Biochem 466 (1/2) (2020) 139–148.
[15] M. Qin, Q. Li, Y. Wang, Rutin treats myocardial damage caused by pirarubicin via regulating miR-22-5p-regulated RAP1/ERK signaling pathway, J. Bioc Hem. Mol. Toxicol. 35 (1) (2021), e22615.
[16] H. Yang, C. Wang, L.Y. Zhang, Rutin alleviates hypoxia/reoxygenation-induced injury in myocardial cells by up-regulating SIRT1 expression, Chem. Bi Ol. Inter. 297 (2019) 44–49.
[17] B.A. Nikfar, M. Adineh, F. Hajjiali, Treatment with rutin-a therapeutic strategy for neutrophil-mediated inflammatory and autoimmune diseases: anti-inflammatory effects of rutin on neutrophils, J. Pharmacopunct. 20 (2017) 52–56.
[18] K. Nemeth, G.W. Plumb, J.G. Berrin, Deglycosylation by small intestinal epithelial cell betaglucosidases is a critical step in the absorption and metabol ism of dietary flavonoid glycosides in humans, Eur. J. Nutr. 42 (2003) 29–42.
[19] M. Teixeiraf, M.N. Coelho, F.D.N. Jose, Oral treatments with a flavonoid-enriched fraction from Cecropia hololeuca and with rutin reduce a rticular pain and inflammation in murine zymosan-induced arthritis, J. Ethnopharmacol. (2020), 112841.
[20] Singhs, D.K. Singh, A. Meena, Rutin protects t-butyl hydroperoxide-induced oxidative impairment via modulating the Nrf2 and iNOS activity, Phyto Med. (55) (2019) 92–104.
[21] F.D. Jin, T. Zhang, Z. Zhang, Protective effect of ruin on oxidative stress injury of HepG2 cells and its machanism[J], JJilin Univ. Med Ed. 46 (6) (2020) 1117–1123, 1345.
[22] X.M. Yang, T.J. Zhang, K.J. Xu, Antioxidant activity comparison of puerarin and other flavonoids in LPS-induced RAW264.7 cells, J. Med Res 44 (11) (2015) 54–56.
[23] M.M. Zhang, Comparison of Antioxidant Capacities and Regulation of Gut Microbiota of Flavonoids, Southwest University, Chongqing, 2018.
[24] X.T. Li, B. Jiang, Y.Y. Wang, Research on the effect of Flos; Sophorae and rutin on scavenging superoxide negion and protecting chondriosome, Inf. Tradit. C. hin Med (6) (2007) 66–68.

[25] Q. Qus, C.C. Dai, H. Guo, Rutin attenuates vancomycin-induced renal tubular cell apoptosis via suppression of apoptosis, mitochondrial dysfunction, an d oxidative stress, Phytother. Res 33 (8) (2019) 2056–2063.
[26] L. Zhang, Y.C. Lai, H.T. Wang, Protective efect of rutin against oxidative injury in neuronal cells, J. Chin. Med Mater. 37 (4) (2014) 640–644.
[27] V.M. Da Rosa, K. Ariotti, C.A. Bressan, Dietary addition of rutin impairs inflammatory response and protects muscle of silver catfish (Rhamdia quele n) from apoptosis and oxidative stress in Aeromonas hydrophila-induced infection, Comp. Biochem Physiol. C. Toxicol. Pharm. (226) (2019), 108611.
[28] Y. Ding, Z.Y. Cao, Kezp, Inhibition of rutin against influenza virus in vitro and its mechanism, Drugs Clin. 30 (12) (2015) 1431–1436.
[29] T.P. Cushniee, A.J. Lamb, Antimicrobial activity of flavonoids, Int J. Antimicrob. Agents 26 (50) (2005) 343–356.
[30] L. Wang, J. Lan, P. Gong, Protective effect of rutin from lios sophorae immaturua on type II diabetes mice, Lishizhen Med Mater. Med Res 28 (2) (2017) 335–338.
[31] H.X. Cao, Z.M. Sun, X.B. Gou, Effect of rutin on myocardial enzyme and cardiac morphology in diabetic mice, Sichuan Univ (Med Sci) 49 (4) (2018) 570–574.
[32] J.H. Miao, J. Bai, J.C. Li, Effect of rutin on renal function and pathological changes in diabetic nephropathy rats[J], Chin. JExp Tradit. Med Form. 21 (13) (2015) 122–125.
[33] Neelam Malik, Priyanka Dhiman, Anurag Khatkar, In silico design and synthesis of targeted rutin derivatives as xanthine oxidase inhibitors, BMC Chem. 13 (2019) 71.
[34] R. Zhou, A. Tardivel, B. Thorens, Thioredoxin-interacting protein links oxidative stress to inflammasome activation, Nat. Immunol. 11 (6) (2010) 136–140.
[35] H.W. Chiu, H. LiL, C.Y. Hsieh, Glucosamine inhibits IL-1 expression by preserving mitochondrial integrity and disrupting assembly of the NLRP3 inflammasome, Sci. Rep. 9 (3) (2019) 5603.
[36] G.L. Wang, H.M. Yuan, Z.F. Wang, Soluble uric acid activates NLRP3 inflammasome in myocardial cells through down-regulating UCP2, J. Sichuan Univ. 49 (1) (2018) 512–517.
[37] Y. Wang, Z.J. Lin, B. Zhang, Cichorium intybus L. extract suppresses experimental gout by inhibiting the NF-κB and NLRP3 signaling pathways, Int. J. Mol. Sci. 20 (19) (2019) 4921.
[38] M. Bian, Z.J. Lin, Y. Wang, Bioinformatic and metabolomics analysis reveal intervention effects of chicory in a quail model of hyperuricemia, Evid. -Based Complement. Altern. Med. (2018), 730385.
[39] B.A. Meng, A. Jw, W.B. Yu, A. An, A. Cz, C. Zs, Chicory ameliorates hyperuricemia via modulating gut microbiota and alleviating lps/tlr4 axis in quail, Biomed. Pharmacother. (2020) 131.
[40] Z. Lin, B. Zhang, X. Liu, R. Jin, W. Zhu, Effects of chicory inulin on serum metabolites of uric acid, lipids, glucose, and abdominal fat deposition in quails induced by purine-rich diets, J. Med. Food 17 (11) (2014) 1214–1221.
[41] H. Wang, Z. Lin, B. Zhang, Preliminary study on the establishment of a quail model of gout induced by high-protein and high-calcium diet combined with restricted drinking water. Chinese Journal of Comparative Medicine 29 (4) (2019) 8, https://doi.org/10.3969/j.issn.1671-7856.2019.04.003.
[42] Y. Wang, M. Chu, W. Li, Z. Lin, B. Zhang, Study on anti-gout disease of traditional Chinese medicines for invigorating spleen and removing dampness based on intestine and kidney axis, World Chin. Med. 16 (01) (2021) 13–19.
[43] E. Smith, D. Hoy, M. Cross, T.R. Merriman, T. Vos, R. Buchbinder, et al., The global burden of gout: estimates from the Global Burden of Disease 2010 study, Ann. Rheum. Dis. 73 (2014) 1470–1476.
[44] D. Bursill, W.J. Taylor, R.Gout Terkeltaub, Hyperuricemia and crystal-associated disease network (G-CAN) consensus statement regarding labels and definitions for disease elements in gout, Arthritis Care Res. (Hoboken) 71 (03) (2019) 427–434.
[45] T.J. Coderre, P.D. Wall, Ankle joint urate arthritis (AJUA) in rats: an alternative animal model of arthritis to that produced by Freund's adjuvant, Pain 28 (1987) 379–393.
[46] A. So, B. Thorens, Uric acid transport and disease, J. Clin. Investig. 120 (06) (2010) 1791–1799.
[47] K. Schroder, J. Tschopp, The Inflammasomes, Cell 140 (2010) 821–832.
[48] J. Pyrzanowska, A. Piechal, K. Blecharz-Klin, I. Joniec-Maciejak, A. Zobel, E. Widy-Tyszkiewicz, Influence of long-term administration of rutin on spatial memory as well as the concentration of brain neurotransmitters in aged rats, Pharm. Rep. 64 (4) (2012) 808–816.
[49] A. Doostkam, H. Mirkhani, K. Iravani, S. Karbalay-Doust, K. Zarei, Effect of rutin on diabetic auditory neuropathy in an experimental rat model, Clin. Exp. Otorhinolaryngol. 14 (3) (2021) 259–267 (Aug).
[50] F.M. Kandemir, M. Ozkaraca, B.A. Yildirim, B. Hanedan, A. Kirbas, K. Kilic, E. Aktas, F. Benzer, Rutin attenuates gentamicin-induced renal damage by reducing oxidative stress, inflammation, apoptosis, and autophagy in rats, Ren. Fail 37 (3) (2015) 518–525 (Apr).
[51] Y. Cai, C. Fan, J. Yan, N. Tian, X. Ma, Effects of rutin on the expression of PPARγ in skeletal muscles of db/db mice, Planta Med. 78 (9) (2012) 861–865 (Jun).
[52] W.A. Ali, W.A. Moselhy, M.A. Ibrahim, M.M. Amin, S. Kamel, E.B. Eldomany, Protective effect of rutin and β-cyclodextrin against hepatotoxicity and nephrotoxicity induced by lambda-cyhalothrin in Wistar rats: biochemical, pathological indices and molecular analysis, Biomarkers 27 (7) (2022) 625–636 (Nov).
[53] C. Tian, Y. Shao, Z. Jin, Y. Liang, C. Li, C. Qu, S. Sun, C. Cui, M. Liu, The protective effect of rutin against lipopolysaccharide induced acute lung injury in mice based on the pharmacokinetic and pharmacodynamic combination model, J. Pharm. Biomed. Anal. 209 (2022), 114480. Feb 5.
[54] S.I. Adachi, M. Oyama, S. Kondo, K. Yagasaki, Comparative effects of quercetin, luteolin, apigenin and their related polyphenols on uric acid production in cultured hepatocytes and suppression of purine bodies-induced hyperuricemia by rutin in mice, Cytotechnology 73 (3) (2021) 343–351 (Jun).